

Tetravalent Colloids by Nematic Wetting

M. HUBER^{1,2} and H. STARK^{1(*)}

¹ *Universität Konstanz, Fachbereich Physik, D-78457 Konstanz, Germany*

² *Department of Physics and Astronomy, University of British Columbia, 6224 Agricultural Road, Vancouver, B.C. V6T1Z1, Canada*

PACS. 82.70.Dd – Colloids.

PACS. 61.30.Hn – Surface phenomena.

PACS. 61.30.Dk – Continuum models and theories of liquid crystal structure.

Abstract. – In an elegant paper, D. Nelson suggested a method to produce tetravalent colloids based on a tetrahedral configuration created on the surface of a spherical particle. It emerges from a two-dimensional nematic liquid crystal placed on a sphere due to the presence of four 1/2 disclinations, i.e., topological defects in the orientational order [1]. In this paper we show that such a tetrahedral configuration also occurs in the wetting layers which form around spheres dispersed in a liquid crystal above the nematic-isotropic phase transition. Nematic wetting therefore offers an alternative route towards tetravalent colloids.

Recently, D. Nelson proposed a method by which tetravalent colloids could be produced [1]. These micron-sized particles would have four chemical linkers or DNA strands symmetrically attached to their surfaces. Similar to, e.g., carbon, silicon and germanium atoms with their sp^3 hybridized chemical bonds, the tetravalent colloids could then arrange into, e.g., a colloidal crystal with a diamond lattice structure which is known to possess a large photonic band gap [2].

To create the attachment sites for the chemical linkers, Nelson considered the two-dimensional nematic liquid crystal phase on the particle surface realized by a monolayer of elongated constituents such as gemini lipids [3], ABA triblock copolymers [4] or nanorods [5]. One could first think that the rodlike particles on a sphere create Mermin's boojums [6], i.e., point defects with topological charge 1 situated at the north and south pole of a sphere as illustrated in Fig. 1a). The lines indicate the director field. A vector order parameter would indeed create such a configuration. The nematic order, however, is described by an axis in space which allows the boojums to split up into a pair of disclinations with charge 1/2. Lubensky and Prost showed that the ground state of a 2D nematic texture on a sphere consists of four 1/2 disclinations situated at the vertices of a tetrahedron [7]. Fig. 1b) tries to illustrate such a configuration with tetrahedral symmetry in the angular space of spherical coordinates, i.e., polar angle θ versus azimuthal angle ϕ . For the moment, let the rectangles symbolize the nematic director. To visualize the boojum configuration in this representation, all the local directors would point along the vertical (lines of longitude). Squares situated on the $\theta = 0, \pi$ line (north and

(*) E-mail: Holger.Stark@uni-konstanz.de

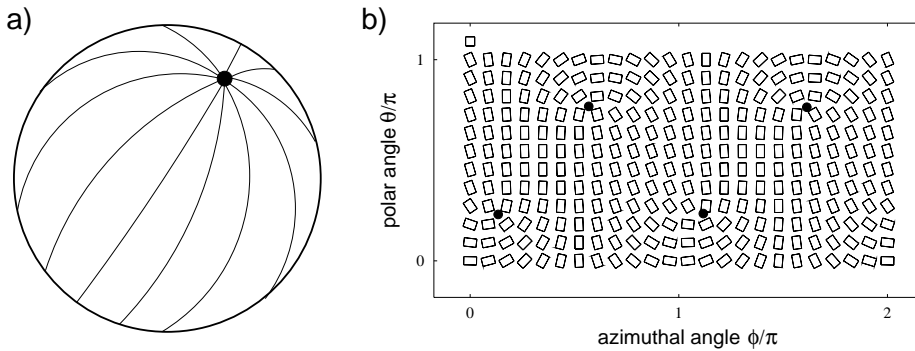


Fig. 1 – Different configurations of a nematic liquid crystal on a sphere. The pictures apply to both a pure two-dimensional nematic and to biaxial nematic wetting layers. a) Boojum configuration with two +1 disclinations at the north and south pole. The lines indicate the director field. b) Tetrahedral configuration visualized in the angular space of spherical coordinates. The orientational order in the sphere is indicated by rectangles. Four +1/2 disclinations (see dots) are located on the vertices of a tetrahedron. As a reference, the square in the upper left corner symbolizes a fully isotropic order of the molecular axis.

south pole) would indicate the isotropic order in the core of the boojums. To arrive at the tetrahedral configuration, the boojums split up into a total of four 1/2 disclinations which move away from the north and south pole as indicated by the dots in Fig. 1b). If one is able to attach chemical linkers selectively to the core of the disclinations, then a tetravalent colloidal chemistry can be realized [1].

Does the tetrahedral configuration survive when the colloid is suspended in the nematic phase of a three-dimensional liquid crystal? The 1/2 disclinations would extend as lines into the solvent. For topological reasons, they have to end either on neighboring particles or at the boundaries of the system. However, the resulting network of defect lines carries a lot of free energy. It can be greatly reduced if the particles realize the boojum configuration. The corresponding +1 defect lines in the bulk nematic phase are not stable and “escape into the third dimension” [8]. This is indeed observed in nematic emulsions [9].

We have recently looked at nematic wetting transitions and capillary condensation in connection with colloids suspended in a liquid crystal solvent above the nematic-isotropic phase transition [10]. So the interesting question arises if the tetrahedral configuration occurs in nematic wetting layers which surround colloidal particles. This would then suggest an alternative route towards tetravalent colloids. In answering the question, one first needs to establish orientational order close to the colloid with a preferred axis parallel to its surface. Since the orientation of the preferred axis should be free to rotate within the surface we cannot just fix it by an appropriate surface potential. All we can do is to favor planar ordering of the liquid crystal molecules at the surface with an isotropic distribution of their axes in the surface. This uniaxial *oblate* order is, however, energetically disfavored in the bulk since close to the phase transition the molecules already have a tendency to align parallel to each other, i. e. to assume uniaxial *prolate* order. As a compromise, biaxial order close to the bounding surfaces occurs and introduces a preferred axis as required. The phase transition from uniaxial oblate to biaxial surface ordering is well studied in literature for planar geometry [11–13]. In the following, we readdress this problem to set the stage for the spherical geometry. For the latter we then show that close to the nematic-isotropic phase transition, the biaxial ordering indeed leads to the tetrahedral configuration as in the two-dimensional case. In addition, we

find that the transition from oblate ordering to the tetrahedral texture occurs via the boojum configuration which possesses a narrow stability region only.

To quantify the surface-induced orientational order, we use a traceless and symmetric second-rank tensor Q_{ij} , also called alignment tensor. We perform our analysis with the help of the Landau-Ginzburg-de Gennes free energy density in the bulk [14], $f(Q_{ij}) = \frac{1}{2}a_0(T - T^*)Q_{ij}Q_{ij} - bQ_{ij}Q_{jk}Q_{ki} + c(Q_{ij}Q_{ij})^2 + \frac{1}{2}L_1(Q_{ij,k})^2 + \frac{1}{2}L_2(Q_{ij,j})^2$ where summation over repeated indices is implied and the symbol $,k$ means spatial derivative with respect to x_k . The first three terms describe the nematic-isotropic phase transition; a_0 and c are positive constants and T^* denotes the supercooling temperature of the isotropic phase. The fourth and fifth term penalize any non-uniform orientational order. Since we are interested in the basic features of our system, we always choose $L_1 = L_2$. The anchoring of the molecules to a bounding surface is quantified by the Nobili-Durand free energy density, $f_S(Q_{ij}) = \frac{W}{2}(Q_{ij} - Q_{ij}^{(0)})^2$, where W is the anchoring strength and $Q_{ij}^{(0)}$ the preferred order parameter at the surface [15]. The number of parameters is reduced by using a rescaled order parameter $\mu_{ij} = Q_{ij}/s$ [$s = b/(\sqrt{6}c)$] and temperature $\tau = 12ca_0(T - T^*)/b^2$. Furthermore, all lengths are given in terms of the particle radius a ($\bar{r} = \mathbf{r}/a$) and the unit of the free energy is $\Delta f a^3 = b^4 a^3 / (36c^3)$. We also introduce the nematic coherence length at the nematic-isotropic phase transition, $\xi_r = (12cL_1/b^2)^{1/2}$, and define the reduced anchoring strength as $\gamma = 6cW/(b^2\xi_r)$ so that the reduced free energy becomes

$$F[\mu_{ij}(\bar{\mathbf{r}})] = \int d^3\bar{r} \left(\frac{1}{4}\tau\mu_{ij}\mu_{ij} - \sqrt{6}\mu_{ij}\mu_{jk}\mu_{kl} + (\mu_{ij}\mu_{ij})^2 + \frac{1}{4}\frac{\xi_r^2}{a^2}[(\mu_{ij,k})^2 + \frac{L_2}{L_1}(\mu_{ij,j})^2] \right) + \frac{\gamma}{2}\frac{\xi_r}{a} \int d^2\bar{r} (\mu_{ij} - \mu_{ij}^{(0)})^2 . \quad (1)$$

Note that in the planar case, we choose $a = \xi_r$ as the unit length. Typical values for the nematic compound 5CB are $\Delta f = 8 \cdot 10^5$ erg/cm³, $\xi_r = 10$ nm, and the temperature interval $\Delta\tau = 1$ corresponds to 1.12 K.

A uniaxial order parameter $\mu_{ij} = \frac{3}{2}S(n_i n_j - \delta_{ij}/3)$, where \mathbf{n} is the nematic director and δ_{ij} the Kronecker symbol, minimizes the first three terms on the right-hand side of Eq. (1). The bulk nematic-isotropic phase transition from $S = 0$ to $S_b = \sqrt{6}/4$ occurs at $\tau_c = 1$, and $\tau^\dagger = 9/8$ is the superheating temperature of the nematic phase. The bulk exhibits prolate order since $S_b > 0$, i.e., the rodlike molecules align along a common axis. In the following, we assume that bounding surfaces favor oblate order. The preferred order parameter at the surface therefore assumes the form $\mu_{ij}^{(0)} = \frac{3}{2}S_0(\hat{\nu}_i \hat{\nu}_j - \delta_{ij}/3)$ with $S_0 < 0$. In general, the order parameter can be biaxial. We visualize it by adding a term proportional to δ_{ij} and by calculating its eigenvectors and eigenvalues whose directions and magnitudes then define the edges of a cuboid. We find that in the planar or spherical geometry one eigenvector always points along the surface normal or the radial direction, respectively. So in Fig. 1b) we only see one face of the cuboid. To test for the biaxiality of μ_{ij} , we introduce the measure [16]

$$B = 1 - 6 \frac{(\mu_{ij}\mu_{jk}\mu_{ki})^2}{(\mu_{ij}\mu_{ij})^3} , \quad (2)$$

which is zero for uniaxial tensors and assumes a maximal value of one. An averaged degree of biaxiality is defined as

$$\bar{B} = \frac{\int d^3\bar{r} \mu_{ij}\mu_{ij} B}{\int d^3\bar{r} \mu_{ij}\mu_{ij}} . \quad (3)$$

It weights the local B with the degree of orientational order given by $\mu_{ij}\mu_{ij}$ such that for $\mu_{ij} \rightarrow 0$ unphysically high local biaxialities do not contribute to \bar{B} .

Stable orientational textures correspond to a minimum of the free energy functional (1). Its variation gives Euler-Lagrange equations for the five independent components of $\mu_{ij}(\bar{\mathbf{r}})$. They are discretized and then solved numerically by the standard Newton-Gauss-Seidel relaxation method using appropriate starting configurations [17]. The planar geometry is just a one-dimensional problem with the bounding surface at $\bar{z} = 0$. To deal with the infinite half space, we introduced a new coordinate $\rho = \exp(-\bar{z})$. Since close to the bulk phase transition the biaxial wetting layer exhibits complete wetting [12], we also used an adaptive grid to resolve the interface between isotropic and orientational order. Oblate and biaxial wetting layers were distinguished by the biaxiality parameter B at the surface. The wetting layers close to a sphere were determined in a spherical coordinate system using the local coordinate basis to define the alignment tensor $\mu_{ij}(\bar{\mathbf{r}})$. We replaced the radial coordinate \bar{r} by $\rho = \exp[-(\bar{r} - 1)a/\xi_r]$ to account for the infinite space around the sphere. The Euler-Lagrange equations were formulated with the help of differential geometry. Phase transitions between different wetting layers were monitored by the averaged biaxiality \bar{B} and by the behavior of the free energy which we calculated numerically by applying Simpson's integration rule to Eq. (1).

We add some comments about the possible orientational textures close to a sphere. It has already been noted that one eigenvector of the tensor order parameter always points along the radial direction. From the remaining eigenvectors, we take the one with the largest eigenvalue as a director. Close to the particle it can then form the *splay* dominated boojum of Fig. 1a) or the *bend* dominated version where the director always points along the lines of latitude of the sphere. Within our numerical accuracy, we observe that both configurations have the same free energy. This is due to the fact that in the Landau-De Gennes theory splay and bend deformations are energetically degenerate. The same applies to the bend dominated tetrahedral configuration of Fig. 1b) and its splay dominated counterpart which follows from Fig. 1b) by rotating all rectangles by 90° . Note that Fig. 1b) illustrates the orientational order a distance of $0.05a$ away from the particle surface. We found that around this distance the biaxiality of the orientational order is the largest. Topological defects in biaxial nematics are more complex than in the uniaxial case [18]. However, since one eigenvector always points along the radial direction, we do not have to worry about these complications and can basically work with the director introduced above to identify the defects.

Before continuing the discussion of the spherical case, we summarize our results for the planar geometry in Fig. 2. We show a phase diagram in terms of temperature τ versus reduced anchoring strength γ , the preferred surface order parameter S_0 is fixed for each transition line. Above $S_0 \approx -1$ only the uniaxial oblate phase exists. For smaller S_0 , a biaxial phase appears at temperatures close to the bulk phase transition ($\tau = 1$) and for sufficiently large anchoring strength. Decreasing S_0 widens the existence region of the biaxial phase. The transition from the uniaxial oblate to the biaxial wetting layer is either of first (solid line) or second (dashed line) order. The transition lines meet in a tricritical point (dot). For large γ , the lines approach a constant temperature $\tau > 1$ (note the logarithmic scale for γ). Our results on a single transition line agree with earlier findings where a one-parameter surface potential with just a surface ordering field was used [12]. With our more realistic surface potential, we show in addition that the biaxial wetting layer only appears for sufficiently small S_0 .

Based on the knowledge of the planar case, we now address the spherical geometry. For 300 nm particles ($a/\xi_r = 30$), Fig. 3a) presents a three-dimensional phase diagram in terms of temperature τ , reduced anchoring strength γ , and preferred order parameter S_0 locating the different types of wetting layers. The phase diagram is the result of extensive numerical calculations which determined the three-dimensional order parameter field close to the particle. They were performed on a PC cluster and would take a few years on a typical state-of-the-art PC. As in the planar case, the uniaxial oblate wetting layer is always stable for $0 < S_0 \leq -1$.

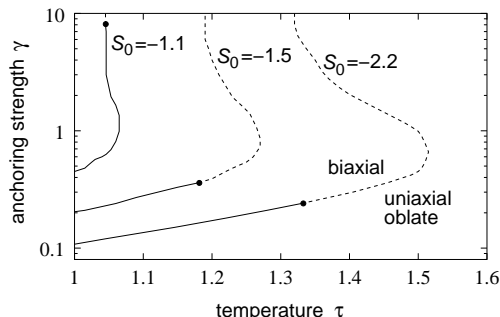


Fig. 2 – Phase diagram for the planar geometry in terms of temperature τ and reduced anchoring strength γ ; the parameter of the curves is the preferred surface order parameter S_0 . First and second-order phase transitions between uniaxial oblate and biaxial wetting layers are indicated by solid and dashed lines, respectively. The dot means tricritical point.

Decreasing S_0 induces first a phase transition to a boojum configuration for sufficiently large γ and then to the tetrahedral wetting layer. Note that the stability region of the boojum is restricted to a very narrow S_0 intervall and, therefore, hardly visible in Fig. 3a). The solid line located on the upper surface indicates a line of tricritical points. To the left of this line, the transition from oblate ordering to the boojum is of first order and to the right it is of second order. In contrast, the transition from the boojum to the tetrahedral configuration is always discontinuous. We never found that the boojum evolves continuously into the tetrahedral configuration via an asymmetric arrangement of the $1/2$ disclinations. One could speculate about the narrow stability region of the boojum configuration. After all, as noted above, in the bulk nematic phase the corresponding $+1$ disclination lines are not stable and “escape into the third dimension” to reduce the free energy. This, however, cannot occur in our case since for the biaxial order parameter the equivalent $+1$ disclination line is actually stable [18]. So the system reduces the free energy by adopting the tetrahedral configuration.

In Fig. 3b) we draw contour lines of the surfaces of the three-dimensional phase diagram for different values of S_0 using the spline function of the graphical program gnuplot. The resulting two-dimensional phase diagrams resemble very much the one in the planar case (see Fig. 2) with the exception that for decreasing temperature, we have a sequence of three phases as indicated for $S_0 = -2$. As before, the solid and dashed lines mean first and second-order transitions, respectively, and the dots show the tricritical points. To account for size effects, we also studied particles with radius $a = 100$ nm ($a/\xi_r = 10$). The phase diagrams in Fig. 4 qualitatively look the same as for the larger particles. Comparing the two-dimensional diagrams of the planar case and the two particle sizes for a fixed S_0 , one clearly recognizes that with increasing curvature the temperature range where the biaxial wetting layers exist becomes smaller. So curvature suppresses the biaxial phases. Surprisingly, the rough location of the transition lines with respect to the anchoring strength γ does not seem to be affected by curvature.

How reasonable are the rescaled parameters of the surface potential where the biaxial wetting layers are observed? Using Landau parameters from 5CB ($b = 0.7 \cdot 10^7$ erg/cm³, $c = 0.5 \cdot 10^7$ erg/cm³) [19] and $\xi_r = 10$ nm, we arrive at $\gamma = W/1 \frac{\text{erg}}{\text{cm}^3}$. So the well achievable anchoring strength $W = 1$ erg/cm³ gives the right order of magnitude for γ . According to the Landau-de Gennes theory, the rescaled bulk nematic order parameter at the phase transition is $S_b = 0.61$ which corresponds to the measured typical value of $S_{mb} = 0.3$ for the Maier-

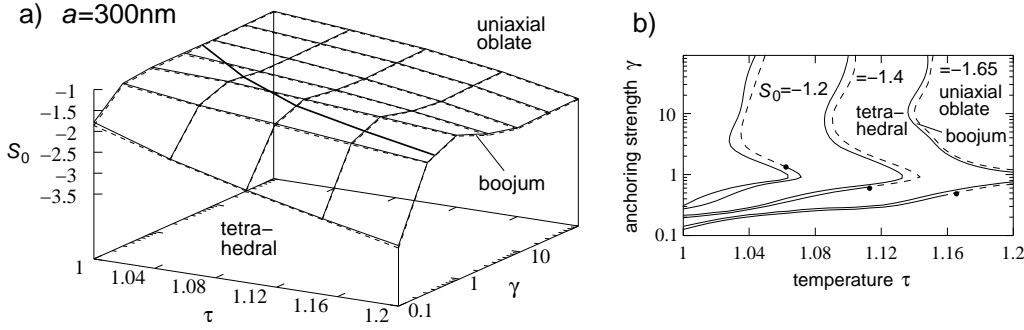


Fig. 3 – a) Three-dimensional phase diagram of the different wetting layers for 300 nm particles. Surface with solid grid lines: transition uniaxial oblate-boojum, surface with dashed grid lines (hardly visible): first-order transition boojum-tetrahedral. The solid line on the upper surface is a tricritical line. It separates a first-order (smaller γ) from a second-order (larger γ) transition. Note the very narrow existence region of the boojum. b) Contour plots of the three-dimensional phase diagram for various S_0 .

Saupe order parameter $S_m = \langle 3 \cos \theta - 1 \rangle / 2$ [20]. For a perfectly aligned nematic (prolate order) $S_m = 1$; the perfect oblate order gives $S_m = -1/2$. This means that in our scaling the minimum value of S_0 in the surface potential is $S_0 = -S_b/S_{mb}/2 = -1.02$. This value is further decreased for smaller S_{mb} , so that our predicted transitions from the oblate to the biaxial surface phases, especially the tetrahedral configuration, should be observable.

Finally, we add some comments about the influence of fluctuations on our phase diagrams. It was argued that in the planar geometry, the transition from the biaxial to the oblate wetting layer is governed by defect unbinding, i.e., by the Berezinskii-Kosterlitz-Thouless (BKT) mechanism [11–13]. As a result, the second-order transition line is shifted to smaller temperatures (see e.g. Ref. [12]). The treatment of fluctuations is beyond the scope of this paper. However, it seems possible that under the BKT mechanism the boojum configuration vanishes completely from the phase diagrams in Fig. 3 and 4 due to its very narrow existence region. In an elaborate and elegant treatment, Nelson finds that the tetrahedral configuration of the two-dimensional nematic is stable against thermal fluctuations deep in the nematic phase, whereas close to the phase transition the fluctuations are fairly large [1]. How these results apply to our studies is not completely clear. It certainly depends on how strong the biaxial ordering is developed in the tetrahedral configuration.

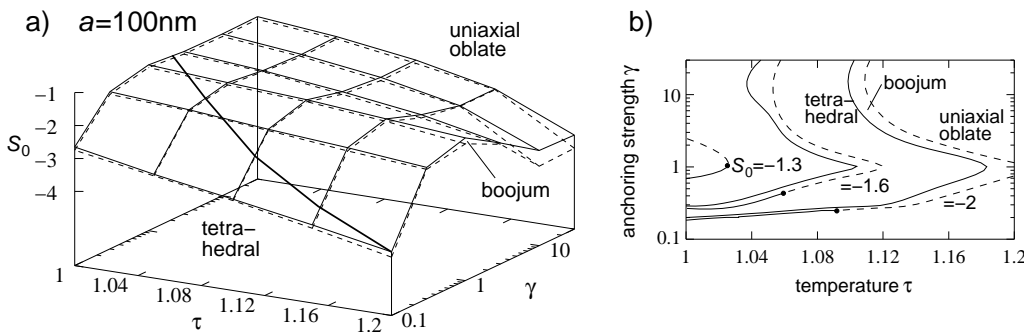


Fig. 4 – The same phase diagrams as in Fig. 3 but now for 100 nm particles.

In conclusion, we have shown that nematic wetting layers around spherical particles possess indeed a tetrahedral configuration where $1/2$ disclinations are located at the vertices of a tetrahedron. This offers an interesting route towards tetravalent colloids. Planar anchoring, necessary for the realization of this tetrahedral configuration, can be realized in inverted nematic emulsions [9], or in lyotropic liquid crystals composed of rodlike surfactant micelles [21]. A possible method to detect nonuniform wetting layers is depolarized light scattering [22]. Furthermore, the Brownian rotational motion of the particles should be measurable by dynamic light scattering [23].

* * *

The authors thank W. Poon for helpful discussions and the Deutsche Forschungsgemeinschaft for financial support under Grant No. Sta 352/5-2 and within the International Graduate College "Soft Matter".

REFERENCES

- [1] NELSON D. R., *Nano Letters*, **2** (2002) 1125.
- [2] HO K. M., CHANG C. T. and SOUKOULIS C. M., *Phys. Rev. Lett.*, **65** (1990) 3152.
- [3] MENGER F. M. and LITTAU C. A., *J. Am. Chem. Soc.*, **115** (1993) 10083.
- [4] SEE, E.G., MATSEN M. W. and SCHICK M., *Macromolecules*, **27** (1990) 187.
- [5] NIKOOBAKHT B., WANG Z. L. and EL-SAYED M. A., *J. Phys. Chem. B*, **104** (2000) 8635; KIM F., KWAN S., AKANA J. and YANG P., *J. Am. Chem. Soc.*, **123** (2001) 4360; LI L., WALDA J., MANNA L. and ALIVISATOS A.P., *Nano Letters (Communication)*, **2** (2002) 557.
- [6] MERMIN N., in *Quantum Fluids and Solids*, edited by S. B. TRICKEY, E. D. ADAMS and J. W. DUFTY (Plenum Press, New York) 1977, pp. 3-22.
- [7] LUBENSKY T.C. and PROST J., *J. Phys. II (France)*, **2** (1992) 371.
- [8] CLADIS P. E. and KLÉMAN M., *J. Phys. (Paris)*, **33** (1972) 591; WILLIAMS C., PIERAŃSKI P., AND CLADIS P. E., *Phys. Rev. Lett.*, **29** (1972) 90; MEYER R. B., *Philos. Mag.*, **27** (1973) 405.
- [9] POULIN P. and WEITZ D. A., *Phys. Rev. E*, **57** (1998) 626.
- [10] FUKUDA J., STARK H. and YOKOYAMA H., *Phys. Rev. E*, **69** (2004) 021714; STARK H., FUKUDA J. and YOKOYAMA H., *Phys. Rev. Lett.*, **92** (2004) 205502.
- [11] SLUCKIN T. J. and PONIEWIERSKI A., *Phys. Rev. Lett.*, **55** (1985) 2907.
- [12] KOTHEKAR N., ALLENDER D. W. and HORNREICH R. M., *Phys. Rev. E*, **49** (1994) 2150.
- [13] HORNREICH R. M., KATS E. I. and LEBEDEV V. V., *Phys. Rev. A*, **46** (1992) 4935; Y. L'VOV, HORNREICH R. M. and ALLENDER D. W., *Phys. Rev. E*, **48** (1993) 1115; SEIDIN R., HORNREICH R. M. and ALLENDER D. W., *Phys. Rev. E*, **55** (1997) 4302.
- [14] DE GENNES P. G., *Mol. Cryst. Liq. Cryst.*, **12** (1971) 193.
- [15] NOBILI M. and DURAND G., *Phys. Rev. A*, **46** (1992) R6174.
- [16] GRAMSBERGEN E. F., LONGA L. and DE JEU W. H., *Phys. Rep.*, **135** (1986) 195.
- [17] PRESS W. H., TEUKOLSKY S. A., VETTERLING W. T. and FLANNERY B. P., *Numerical Recipes in Fortran: The Art of Scientific Computing* (Cambridge University Press, Cambridge) 1992.
- [18] TOULOUSE G., *J. Phys. (Paris) Lett.*, **38** (1977) L67; MERMIN N. D., *Rev. Mod. Phys.*, **51** (1979) 591; KLEMAN M. and LAVRETOVICH O., *Soft Matter Physics* (Springer, Berlin) 2001
- [19] COLES H. J., *Mol. Cryst. Liq. Cryst.*, **49** (1978) 67.
- [20] DE GENNES P. G. and PROST J., *The Physics of Liquid Crystals* (Oxford Science Publications, Oxford) 1993
- [21] POULIN P., FRANCÈS N. and MONDAIN-MONVAL O., *Phys. Rev. E*, **59** (1999) 4384
- [22] BERNE B. J. and PECORA R., *Dynamic Light Scattering – with applications to chemistry, biology, and physics* (John Wiley, New York) 1976
- [23] MERTELJ A., ARAUZ LARA J. L., MARET G., GISLER T. and STARK H., *Europhys. Lett.*, **59** (2002) 337.